# Design of Space Vector-Based Hybrid PWM Techniques for Reduced Current Ripple

H. Krishnamurthy, G. Narayanan, R. Ayyanar
Department of Electrical Engineering
Arizona State University, Tempe, USA

V.T. Ranganathan
Department of Electrical Engineering
Indian Institute of Science, Bangalore, India

***Abstract* – Switching sequence used by conventional space vector PWM (CSVPWM) involves equal division of zero vector time between the two zero states in every subcycle. The sequences employed by bus-clamping PWM involve use of only one zero state in a subcycle. This paper deals with two sequences, which use only one zero state and involve division of active vector time within a subcycle. A novel hybrid PWM technique, employing these two sequences in conjunction with the conventional sequence, is proposed. The proposed PWM technique is designed using the notion of stator flux ripple. A procedure is presented for designing hybrid PWM techniques involving multiple sequences for reduced current ripple. The proposed PWM technique results in reduced current ripple over CSVPWM at higher modulation indices. Experimental results on a 2hp prototype induction motor drive are presented.**

## I. INTRODUCTION

Real-time PWM techniques for voltage source inverter fed induction motor drives work on the principle of volt-second balance. The reference voltage commanded by the controller is met by the PWM inverter in an average sense over the given sampling period or subcycle [1-8].

Two popular approaches to real-time PWM generation are the Triangle Comparison (TC) approach and the Space Vector (SV) approach. The division of zero vector time between the two zero states in the SV approach is equivalent to addition of triplen frequency components to the three phase modulating waves in the TC approach [4]. However, division of active vector time, which is possible with the SV approach, has no equivalence in the TC approach. Thus, the SV approach is more general than the TC approach [5,6].

Section II presents different possible switching sequences used in the space vector approach. These include two sequences involving division of active vector time. Section III analyzes the different sequences using the notion of stator flux ripple. Section IV presents the design of novel hybrid PWM technique employing the above two sequences in conjunction with conventional sequence. Experimental results are presented in section V, while conclusions are presented in section VI.

## II. SWITCHING SEQUENCES

The voltage vectors, produced by a three-phase inverter, divide the space vector plane into six sectors as shown in Fig. 1. As the sectors are symmetric, the discussion here is limited to sector I alone. In the space vector approach to PWM, an average vector equal to the sample of the reference vector is generated in every subcycle or sampling period $T_S$.

This work was partly funded by the Office of Naval Research, USA under contract N00014-02-1-0751.

Given a commanded vector of magnitude $V_{REF}$ and angle $\alpha$ in sector I as shown in Fig. 1, the volt-second balance is maintained by applying the active state *1*, the active state *2* and the two zero states together for durations $T_1$, $T_2$ and $T_Z$, respectively, as given in (1).

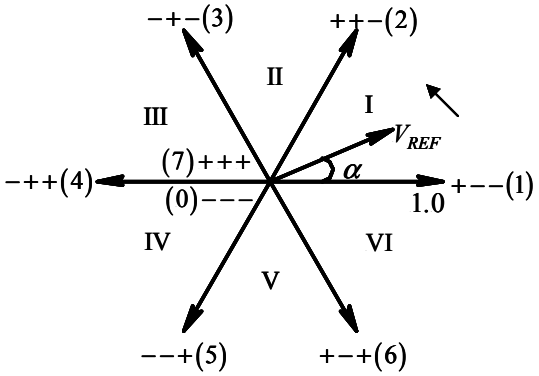


Fig. 1. Switching states and corresponding voltage vectors of a three-phase converter. I, II, III, IV, V and VI are sectors

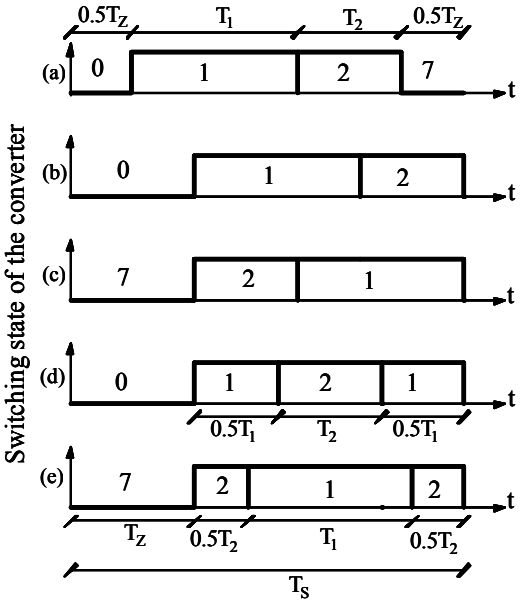


Fig. 2. Different possible switching sequences in a subcycle.

$$T_1 = V_{REF}\frac{\sin(60^\circ-\alpha)}{\sin(60^\circ)}T_S$$

$$T_2 = V_{REF}\frac{\sin(\alpha)}{\sin(60^\circ)}T_S$$

$$T_Z = T_S - T_1 - T_2 \quad \text{... (1)}$$

Different switching sequences can be used within the subcycle to generate the given average vector as shown in Fig. 2. The conventional sequence *0127* applies both the zero states for equal durations of time. The clamping sequences *012* and *721* use only one zero state. This results in the clamping of the B-phase to the negative DC bus (if the zero state *7* is avoided), or of the R-phase to the positive DC bus (if the zero state *0* is avoided) [1-8]. Also, either the active state *1* or active state *2* can be applied twice within the same subcycle as shown in Fig. 2. Thus, sequence *0121* or *7212* can also be used to generate the given average vector with either $T_1$ or $T_2$ divided into two equal halves [5,6]. While the first two types of sequences have been extensively used in the literature [1-8], very little attention has been paid to the last two types of sequences [1,5,6]. This paper analyses the effect of these sequences on the line current ripple, and proposes a new hybrid PWM technique using these two sequences along with the conventional sequence.

## III. ANALYSIS BASED ON STATOR FLUX RIPPLE

The applied voltage vector equals the reference voltage vector only in an average sense over the given subcycle, and not in an instantaneous fashion. The difference between the reference vector and the instantaneous applied voltage vector is the instantaneous error voltage vector. The time integral of the error voltage vector, referred to as 'stator flux ripple vector', is a measure of the ripple in the line current [6]. Time integral of error voltage has been widely used for analysis of PWM techniques [4,6-8]. It is used for design of hybrid PWM techniques here.

At any instant within a given subcycle, one of the two active vectors or the zero vector is applied. When the zero vector is applied, the error voltage vector is equal to the negative of the average vector to be generated. When an active vector is applied, the error voltage vector is the vector originating from the tip of the average vector and ending at the tip of the active vector applied. Volt-second balance ensures that the stator flux ripple vector starts and ends with zero magnitude in every subcycle.

The error vector can be resolved in a synchronously revolving d-q reference frame as shown in Fig. 3. The stator flux ripple vector corresponding to sequences *0127, 0121* and *7212* for a given reference vector are shown in Figs. 3a, 3b

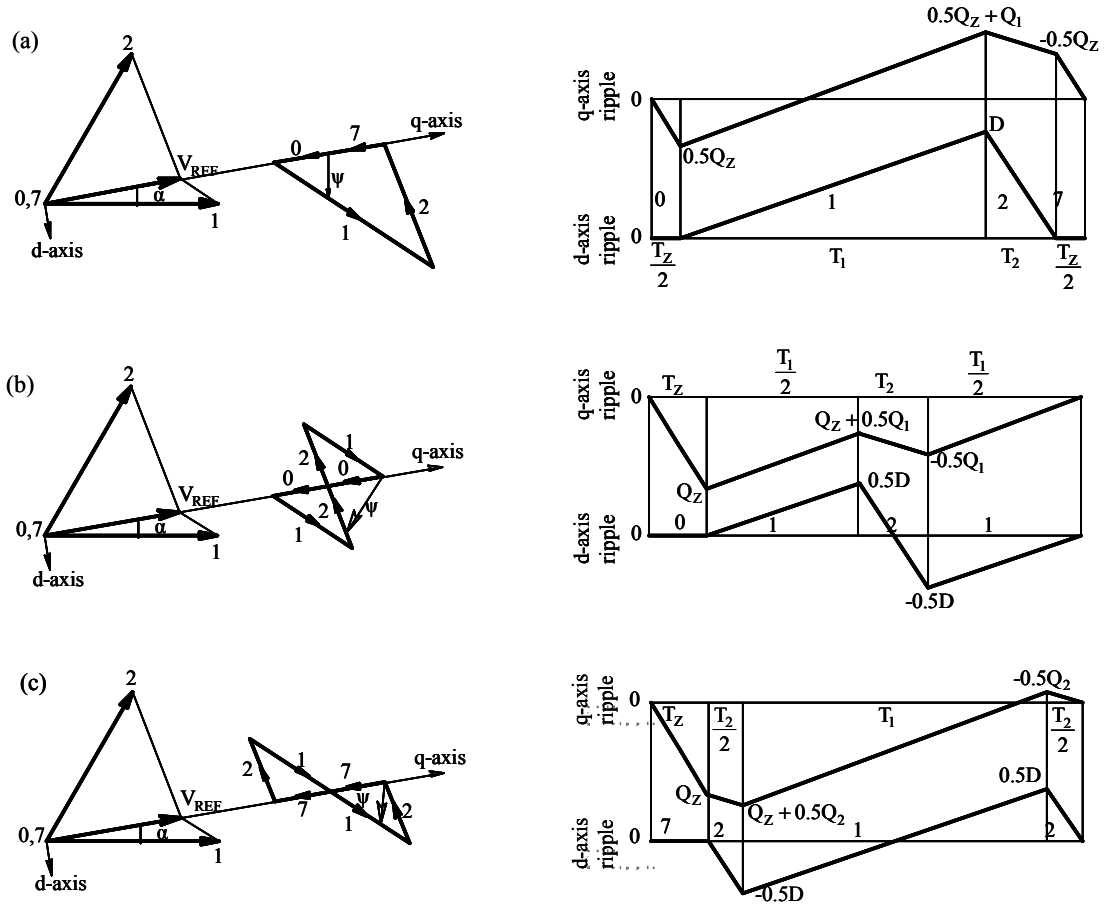


Fig. 3. Stator flux ripple for sequences (a) *0127,* (b) *0121* and (c) *7212*

and 3c, respectively. The d-axis and the q-axis components of the flux ripple vector are also shown. The values of q-axis ripple at the switching instants are given in terms of $Q_Z$, $Q1$ and $Q_2$, while those of d-axis ripple are given in terms of $D$. The quantities $Q_Z$, $Q_1$, $Q_2$ and $D$ are as defined in (2).

$$\begin{aligned} Q_Z &= -V_{REF} T_Z \\ Q_1 &= [\cos(\alpha) - V_{REF}]\, T_1 \\ Q_2 &= \left[\cos(60^\circ - \alpha) - V_{REF}\right] T_2 \\ D &= \sin(\alpha)\, T_1 \end{aligned} \qquad \ldots(2)$$

The mean square value of the stator flux ripple vector gives a measure of the distortion in the line currents. From Fig. 3a the expression for mean square ripple over a subcycle for sequence *0127* can be obtained as shown in (3). Similar expressions for *0121* and *7212* can be derived from Figs. 3b and 3c, respectively, as shown in (4) and (5).

$$\begin{aligned} F_{0127}^2 &= \frac{1}{3}(0.5Q_Z)^2 \frac{T_Z}{2T_S} + \frac{1}{3}\left[\begin{matrix}(0.5Q_Z)^2 + 0.5Q_Z(0.5Q_Z + Q_1) \\ +(0.5Q_Z + Q_1)^2\end{matrix}\right]\frac{T_1}{T_S} \\ &+ \frac{1}{3}\left[(0.5Q_Z + Q_1)^2 - (0.5Q_Z + Q_1)0.5Q_Z + (-0.5Q_Z)^2\right]\frac{T_2}{T_S} \\ &+ \frac{1}{3}(-0.5Q_Z)^2 \frac{T_Z}{2T_S} + \frac{1}{3}D^2 \frac{(T_1 + T_2)}{T_S} \end{aligned} \qquad \ldots(3)$$

$$\begin{aligned} F_{0121}^2 &= \frac{1}{3}Q_Z^2 \frac{T_Z}{T_S} + \frac{1}{3}\left[Q_Z^2 + Q_Z(Q_Z + 0.5Q_1) + (Q_Z + 0.5Q_1)^2\right]\frac{T_1}{2T_S} \\ &+ \frac{1}{3}\left[(Q_Z + 0.5Q_1)^2 - (Q_Z + 0.5Q_1)0.5Q_1 + (-0.5Q_1)^2\right]\frac{T_2}{T_S} \\ &+ \frac{1}{3}(-0.5Q_1)^2 \frac{T_1}{2T_S} + \frac{1}{3}(0.5D)^2 \frac{(T_1 + T_2)}{T_S} \end{aligned} \qquad \ldots(4)$$

$$\begin{aligned} F_{7212}^2 &= \frac{1}{3}Q_Z^2 \frac{T_Z}{T_S} + \frac{1}{3}\left[Q_Z^2 + Q_Z(Q_Z + 0.5Q_2) + (Q_Z + 0.5Q_2)^2\right]\frac{T_2}{2T_S} \\ &+ \frac{1}{3}\left[(Q_Z + 0.5Q_2)^2 - (Q_Z + 0.5Q_2)0.5Q_2 + (-0.5Q_2)^2\right]\frac{T_1}{T_S} \\ &+ \frac{1}{3}(-0.5Q_2)^2 \frac{T_2}{2T_S} + \frac{1}{3}(0.5D)^2 \frac{(T_1 + T_2)}{T_S} \end{aligned} \qquad \ldots(5)$$

## IV. PROPOSED HYBRID PWM TECHNIQUE

It is proposed to design a hybrid PWM technique, employing sequences *0127, 0121* and *7212*, which results in less ripple current than CSVPWM at a given average inverter switching frequency.

As shown in the previous section, for a given average vector the mean square ripple over the given subcycle depends on the switching sequence employed. Given a set of possible sequences, the one that results in the lowest mean square ripple for the given reference vector must always be employed. The design of hybrid PWM technique for reduced current ripple involves determination of zones of superior performance for every sequence. The zone of superior performance for a given sequence is the spatial zone within a sector where the given sequence results in less RMS ripple than the other sequences considered.

The mean square ripple over a subcycle for any sequence is a function of $V_{REF}$, $\alpha$ and $T_S$. Since, all three sequences

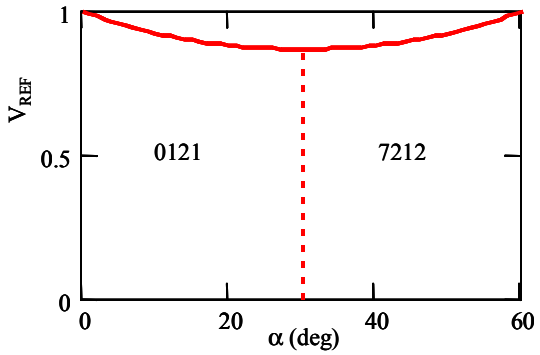


Fig. 4. Comparison of sequences 0121 and 7212 - zones of superior performance

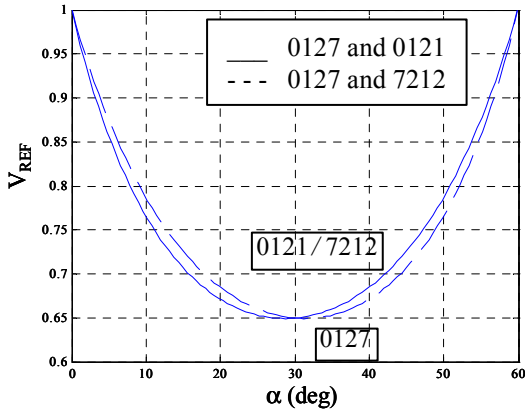


Fig. 5. Comparison of 0121 and 7212 against 0127 - zones of superior performance

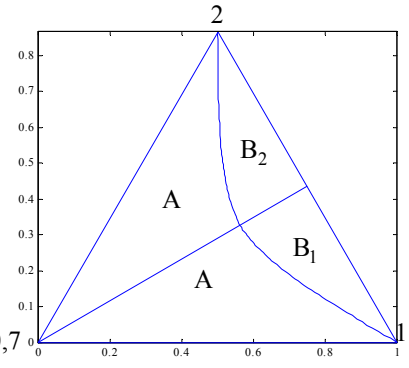


Fig. 6. Proposed hybrid PWM technique
Zone A : Sequences 0127, 7210, ...
Zone $B_1$ : Sequences 0121, 1210, ...
Zone $B_2$ : Sequences 7212, 2127, ...

involve three switchings per subcycle, the same subcycle duration, $T_S$ may be considered for all three. In case the number of switchings is different for different sequences, the subcycle duration must be maintained proportional to the number of switchings per subcycle.

*A. Comparison of 0121 and 7212*

Comparing the expressions given in (4) and (5), it can be seen that the mean square ripple produced by *0121* and *7212* are equal at $\alpha = 30^0$ for any value of $V_{REF}$. However, for $\alpha < 30^0$, *0121* results in less ripple than *7212*. For $\alpha > 30^0$, *7212* produces less ripple than *0121*. This is shown in Fig. 4.

*B. Comparison of 0127 and 0121*

From (3) and (4), the zones of superior performance of *0127* and *0121* can be identified. Sequence *0121* results in less ripple in the spatial region above the solid line in Fig. 5, while *0127* results in less ripple below the solid line.

*C. Comparison of 0127 and 7212*

From (3) and (5), the zones of superior performance of *0127* and *7212* can be identified. Sequence *7212* leads to less ripple in the spatial region above the dashed line in Fig. 5, while *0127* results in less ripple below the dashed line.

D. *Comparison of 0127, 0121 and 7212*

Figs. 4 and 5 together give a comparison of the sequences *0127, 0121* and *7212.* The region above the solid line in the left half of Fig. 5 is the zone of superior performance of *0121*. The region above the dashed line in the right half of Fig. 5 is the zone of superior performance of *7212*. The remaining spatial region is the zone of superior performance of *0127*.

Fig. 6 shows the proposed hybrid PWM technique. The zones of superior performance of sequences *0127, 0121* and *7212* are shown in the space vector plane as A, $B_1$ and $B_2$, respectively. Sequences *0127* and *7210* are used in alternate subcycles in zone A. Sequences *0121* and *1210*, and sequences *7212* and *2127* are used in alternate subcycles in zones $B_1$ and $B_2$, respectively.

*E. Generalized design procedure*

The above procedure can be generalized for design of such hybrid PWM techniques, employing any given set of sequences. The procedure involves the following steps:

- Consider subcycle duration proportional to the number of switchings per subcycle for every sequence. (For example, $T_S = T$ for sequences with three switchings per subcycle, and $T_S = 2T/3$ for sequences with two switchings per subcycle.)

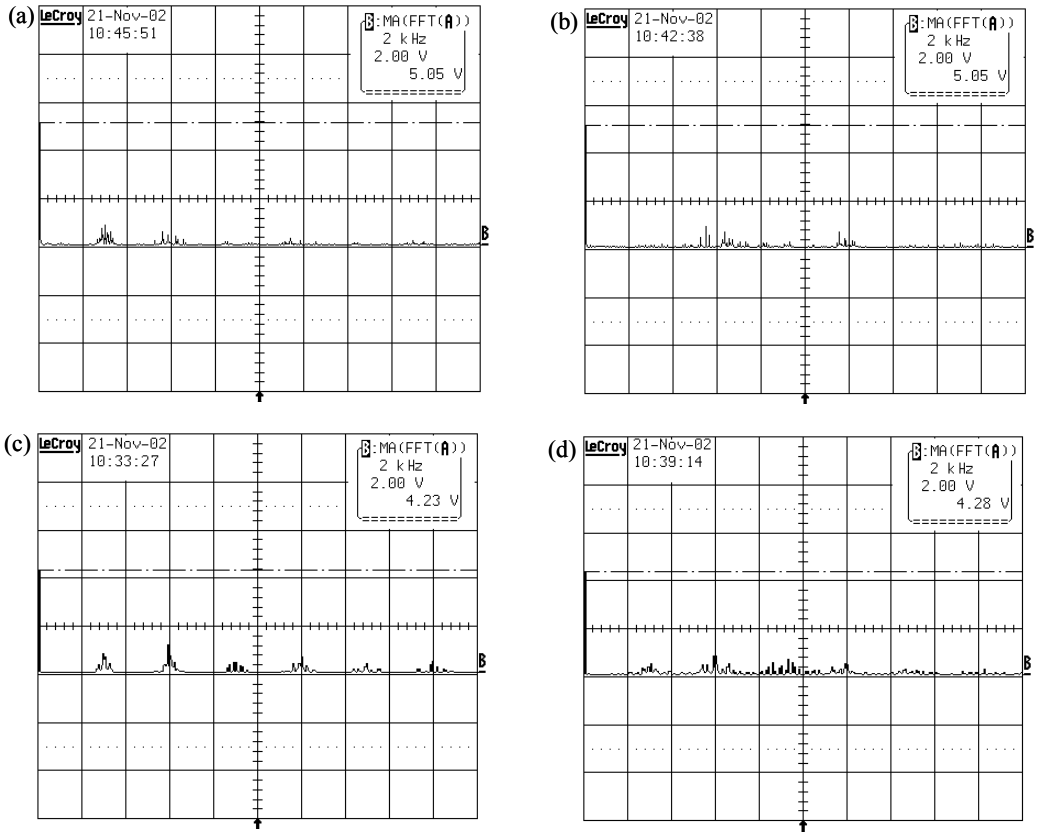


Fig. 7. Measured spectra of line-line voltage (PWM of R-phase minus PWM of Y-phase) for (a) CSVPWM at $V_{REF} = 0.866$ $F_1 = 60$Hz, (b) proposed PWM at $V_{REF} = 0.866$, $F_1 = 60$Hz, (c) CSVPWM at $V_{REF} = 0.722$, $F_1 = 50$Hz and (d) proposed PWM at $V_{REF} = 0.722$, $F_1 = 50$Hz. Switching frequency is 3kHz for (a) to (d).

- Sketch the stator flux ripple trajectory over a subcycle for every sequence.
- Derive the expression for mean square ripple over a subcycle for every sequence.
- Identify the zone of superior performance for every sequence using the above expressions.

## V. EXPERIMENTAL RESULTS

The proposed PWM technique is tested on a 3kVA inverter fed 2hp, 230V, 60Hz induction motor drive. TMS320F243 DSP evaluation module is used as the controller platform.

Figs. 7a and 7b present the measured spectra of line voltage for conventional space vector PWM and proposed hybrid PWM, respectively, at a fundamental frequency of 60Hz and average switching frequency of 3kHz. Figs. 7c and 7d present similar spectra at a fundamental frequency of 50Hz and the same switching frequency as above.

The experimental no-load current waveforms,

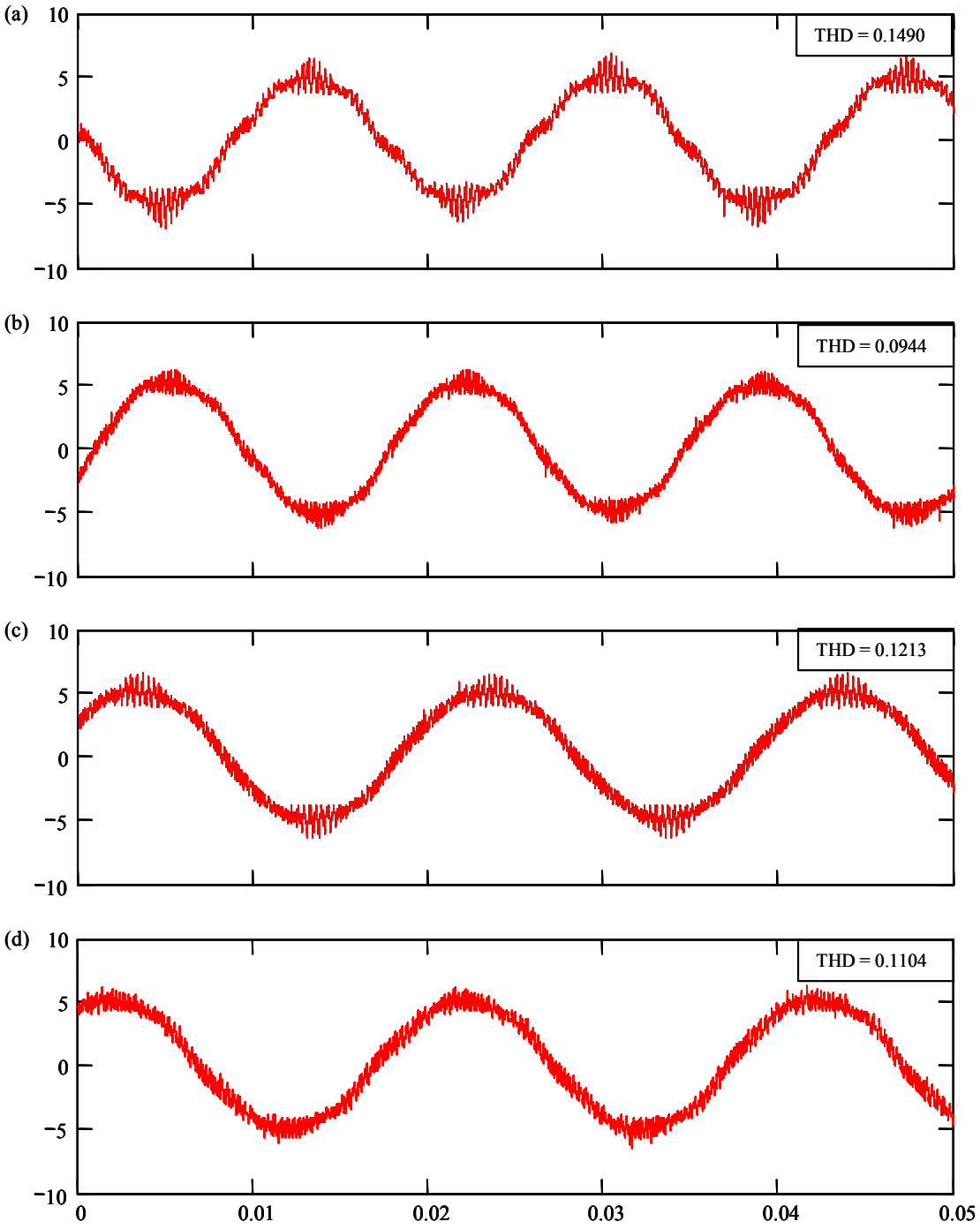


Fig. 8. Measured no-load current in amperes for (a) CSVPWM at $F_1$=60Hz, (b) proposed hybrid PWM at $F_1$=60Hz, (c) CSVPWM at $F_1$=50Hz and (d) proposed hybrid PWM at $F_1$=50Hz

corresponding to the spectra in Figs. 7a to 7d, are shown in Figs. 8a to 8d, respectively.

The total harmonic distortion factor of the no-load current ($I_{THD}$) is widely used as a performance index for PWM techniques. $I_{THD}$ is defined in (6), where $I_1$ is the RMS fundamental no-load current and $I_n$ is the RMS $n^{th}$ harmonic current.

$$I_{THD} = \frac{1}{I_1}\sqrt{\sum_{n\neq 1} I_n^2} \quad \text{... (6)}$$

The measured $I_{THD}$ values are shown along with the current waveforms in Figs. 8a to 8d.

## VI. CONCLUSION

A hybrid PWM technique using two switching sequences, involving division of active vector time, and the conventional sequence is proposed. The maximum line voltage obtainable for a given dc bus voltage with the proposed technique is as high as conventional space vector modulation. For a given inverter average switching frequency, the proposed technique results in significant reduction in harmonic distortion at higher speeds of the induction motor drive. Experimental results on a 2hp induction motor drive are presented.

## REFERENCES


[1] J.Holtz, "Pulsewidth modulation – a survey," *IEEE Trans. IE,* vol. 39(5), pp. 410-420, 1992.

[2] S. Ogasawara, H. Akagi and A. Nabae, "A novel PWM scheme of voltage source inverters based on space vector theory," *3rd European Conference on Power Electronics and Applications, EPE'89*, Aachen, Germany, pp. 1197-1202, Oct 1989.

[3] J.W.Kolar, H.Ertl, F.C.Zach, "Minimising the current harmonics RMS value of three-phase PWM converter system by optimal and suboptimal transition between continuous and discontinuous modulation," in *Conf. Rec. IEEE-PESC '91*, USA, June 1991, pp.372-381.

[4] A.M.Hava, R.J.Kerkman, T.A.Lipo, "Simple analytical and graphical methods for carrier-based PWM-VSI drives," *IEEE Trans. PE*, vol. 14(1), 1999, pp. 49-61.

[5] G.Narayanan, V.T.Ranganathan, "Synchronised PWM strategies based on space vector approach. Part 1: Principles of waveform generation," *IEE Proc.–Electr. Power Appl*, vol. 146(3), 1999, pp. 267-275.

[6] G. Narayanan, "Synchronised pulsewidth modulation strategies based on space vector approach for induction motor drives," Ph.D. Thesis, Indian Institute of Science, Bangalore, India, Aug. 1999.

[7] H.W. van der Broeck, "Analysis of the harmonics in voltage fed inverter drives caused by PWM schemes with discontinuous switching operation," *4th European Conference on Power Electronics and Applications, EPE'91,*Firenze, Italy, pp. 261-266, 1991.

[8] S. Fukuda and K. Suzuki, "Harmonic evaluation of two-level carrier-based PWM methods," *7th European Conference on Power Electronics and Applications, EPE'97*, Trondheim, pp. 331-336, 1997.